Research & Reviews: Journal of Pharmacy and Pharmaceutical Sciences e-ISSN: 2320-1215

Molecular Model of Inhibition of the Catalytic Fragment of Domain ExoN of Exoribonuclease of Virus SARS-CoV-2-Betacoronavirus B by Drug FS-1 Containing Molecular Iodine and Lithium and Magnesium Halides

Gulnara Abdrashidovna Yuldasheva[1]*, Ilya Sergeevich Korotetskiy[1], Kaissar Tabynov[2], Kairat Tabynov[2], Aleksandr Ivanovich Ilin[1]

[1]Scientific Center for Anti-infectious Drugs, Street Al-Farabi 75b, Almaty, Kazakhstan

[2]International Center for Vaccinology, Abay Avenue 8, Almaty, Kazakhstan

Research Article

Received: 05-Jun-2024, Manuscript No. JPPS-24-138328; **Editor assigned**: 07-Jun-2024, PreQC No. JPPS-24-138328 (PQ); **Reviewed:** 21-Jun-2024, QC No. JPPS-24-138328; **Revised:** 28-Jun-2024, Manuscript No. JPPS-24-138328 (R); **Published:** 08-Jul-2024,
DOI: 10.4172/2320-1215.13.3.001

***For Correspondence:**
Gulnara Abdrashidovna Yuldasheva, Scientific Center for Anti-Infective Drug, Street Al-Farabi 75b, Almaty, Kazakhstan
E-mail: yuldasheva57@rambler.ru

Citation: Yuldasheva GA, et al. Molecular Model of Inhibition of the Catalytic Fragment of Domain ExoN of Exoribonuclease of Virus SARS-CoV-2-Betacoronavirus B by Drug FS-1 Containing Molecular Iodine and Lithium and Magnesium Halides. RRJ Pharm Pharm Sci. 2024;13:001

ABSTRACT

Model of inhibition of the catalytic fragment of domain ExoN of exoribonuclease of virus SARS-CoV-2-betacoronavirus B by Drug FS-1 containing molecular iodine and lithium and magnesium halides was proposed by the molecular modeling method.

For the genome of the virus taken from isolate of SARS-CoV-2/INMI1/human/2020/ITA, the frequency of occurrence of nucleotide triplets has been analysed. The most common triplet is AAA (281).

Using the DFT/B3PW91/6-31G** approach, it is shown the active complexes of drug FS-1: $(MgI_3LiII_2)^+$ and $Li(Cl)I_3$, can segregate from the dextrin helix and can form a complex with donor-active atoms of the triplet AAA of viral RNA.

Complexes of active center of nanocomplex FS-1 with triplet AAA destroy the complex formed by a phosphate group of viral RNA and a catalytic fragment of domain ExoN of exoribonuclease and form a new nucleoprotein complex where lithium chloride and $(MgI_3LiII_2)^+$ bind both viral RNA and magnesium ions of the catalytic fragment of domain ExoN of exoribonuclease. The conditions of cleavage of RNA are violated.

The drug FS-1 substance has virus inhibitory activity at a concentration of 3.36 mg/ml in Vero E6 cell culture against coronavirus infection COVID-19 (strain hCoV19/Kazakhstan/KazNAU-NSCEDI-481/2020) in a dose of 100 TCID50/0.2 ml. Result of experimental research and the proposed

molecular model show that the nanocomplex of drug FS-1 have anticoronavirus effect.

Keywords: Coronaviruses; Exoribonuclease; Iodine complex; Magnesium and lithium halides; Nanocomplex; Quantum-chemical DFT approach

INTRODUCTION

The 2020 pandemic has clearly shown the relevance of creating antiviral drugs. One of the targets of the drug is the active center of the vital enzymes of the virus [1,2]. Such drugs include the antibacterial [3] and antiviral [4-5] drug FS-1 [6].

In our earlier articles [7-9], we showed that the active substance of the drug FS-1 is a nanocomplex of dextrin with magnesium and lithium halides and molecular iodine. The active centers of the drug FS-1 are inside the dextrin helix: Binuclear complex of magnesium and lithium containing molecular iodine and triiodide $(MgI_3LiII_2)^+$, a complex of molecular iodine and lithium halide ($(Li(Cl)I)I_2$) and triiodide (I_3^-). The polypeptide located outside the dextrin helix forms a hydrogen bond with the dextrin, and coordinates molecular iodine being a part of the binuclear complex $(MgI_3LiII_2)^+$.

The molecular iodine in drug FS-1 is in particular electronic form, which minimizes its toxic effects in human organism, so the drug FS-1 can be used for parenteral and oral use.

SARS-CoV-2 is an enveloped, positive-sense (+), singlestranded RNA betacoronavirus with a 30 Kilobase (kb) genome [10]. Upon infection of host cells, the SARS-CoV-2 genomic RNA (gRNA) serves as an mRNA template decoded to produce the viral Nonstructural Proteins (NSPs) essential for replication [11,12].

Coronaviruses express Exoribonuclease (ExoN), which is nonstructural protein nsp14. The enzyme is necessary for accuracy of the replication, and is highly conservative within the genus. All the biochemical and genetic data prove that nsp14 is necessary for reading RNA. The RNA sequence encoding nsp14 is responsible for sensitivity to mutagens [13,14].

In article have shown that engineered inactivation of Severe Acute Respiratory Syndrome (SARS)-CoV-2 ExoN activity results in a stable mutator phenotype with profoundly decreased fidelity *in vivo* and attenuation of pathogenesis in young, aged and immunocompromised mice. The ExoN inactivation genotype and mutator phenotype are stable and do not revert to virulence, even after serial passage or long-term persistent infection *in vivo*. ExoN inactivation has potential for broad applications in the stable attenuation of CoVs and, perhaps, other RNA viruses.

A crystal of nsp14 protein has been obtained as a complex with its activator, nonstructural protein (nsp10) and functional ligands for virus SARS-CoV-2-betacoronavirus B, which is responsible for the pandemic of a new type of pneumonia in 2020 [15]. It is shown that one molecule of nsp10 interacts with nsp14 to stabilize and stimulate its activity. The crystalline structure of Exoribonuclease domain (ExoN) of protein nsp14 is presented. The structure of catalytic nucleus of domain ExoN simulates the structures of the catalytic domain of super-family exonucleases such as e-sub-unit of DNA polymerase III of *E. coli*. The catalytic fragment of these polymerases contains two Mg^{2+} ions combined by DEDDh motif consisting of five amino acid residues [16,17].

In the crystalline structure of the catalytic fragment of domain ExoN, only one Mg^{2+} ion is found, which is coordinated by amino acid residues aspartic and glutamine acid, and the second magnesium ion is not found. This is due to the fact that two magnesium ions in domain ExoN are not bound into the binuclear complex and are bound in the binuclear complex only when they interact with a phosphate group of RNA.

In this article antiviral activity, the drug FS-1 against coronavirus COVID-19 *in vitro* is determined according to therapeutic, prophylactic and virus inhibition scheme.

It is shown that the drug FS-1 substance has virus inhibitory activity at a concentration of 3.36 mg/ml in Vero E6 cell culture against coronavirus infection COVID-19 (strain hCoV19/Kazakhstan/KazNAU-NSCEDI-481/2020) in a dose of 100 TCID50/0.2 ml.

Using a method of molecular modeling it is proposed a model of inhibition of magnesium ions of the catalytic fragment of domain ExoN by the active centers nanocomplex of the drug FS-1, a complex of molecular iodine with lithium halide ($(Li(Cl)I)I_2$) and binuclear complex of magnesium and lithium with molecular iodine and triiodide $(MgI_3LiII_2)^+$.

Complexes of active center of nanocomplex FS-1 with triplet AAA (the most common triplet) destroy the complex formed by a phosphate group of viral RNA and a catalytic fragment of domain ExoN of exoribonuclease, and form a new nucleoprotein complex where lithium chloride and $(MgI_3LiII_2)^+$ bind both viral RNA and magnesium ions of the catalytic fragment of domain ExoN of exoribonuclease. The conditions of cleavage of RNA are violated.

MATERIALS AND METHODS

Structures modeling the mechanism anticoronavirus effect of drug FS-1 are calculated using DFT/B3PW91/6-31G** approach. Total energies of the complexes in aqueous solution calculated using model COSMO [18]. Calculations were carried out using the Gaussian 09 [19].

The antiviral activity of the FS-1 against COVID-19 *in vitro* is determined based on therapeutic, prophylactic and virus inhibition schemes.

For the study, a coronavirus cell culture line was used. The VERO C1008 cell culture (Vero 76, clone E6, Vero E6) (ATCC® CRL1586™) was adapted for use in the COVID-19 model. Storage, propagation (including environmental conditions), viability and growth controls of the coronavirus cell culture line VERO C1008 (Vero 76, clone E6, Vero E6) (ATCC® CRL1586™) were conducted in accordance with the ATCC product sheet.

Strain hCoV-19/Kazakhstan/KazNAU-NSCEDI-481/2020 of SARS-CoV-2 virus (COVID19; strain number 481) belongs to family *Coronaviridae*, genus *Betacoronavirus*. The strain was isolated at the NSCEDI named after Aikimbayev M, in Biosafety Level 3 (BSL-3) laboratory in June 2020 from nasopharyngeal swabs taken from people with suspected SARS-CoV-2 infection in Almaty. The strain was cultured in Vero E6 cell culture and PCR detected the N-gene of SARS-CoV-2 virus. Genetic feature of the strain: Mutation *D614G* protein S; the full sequence of the protein was published in the GISAID database under number EPI_ISL_514093. The infectivity of the strain in Vero E6 cell culture is 6.00 lg TCID50/cm^3. The strain is intended for preparation and testing of immunobiological preparations (diagnostic test systems, immunoglobulins and vaccines) and for determination of antiviral activity of various substances *in vitro* and *in vivo*. Method, conditions and composition of media for strain storage: In native form at minus 80°C, culture suspension of Vero E6 cell culture, with DMEM medium+2% Fetal Bovine Serum (FBS)+Antibiotic-Antimycotic solution (Anti-anti; 1x). Method, conditions and composition of media for strain multiplication in Vero E6 cell culture: DMEM medium+2% FBS+Anti-anti (1x) at (37°C ± 0.1°C).

Antiviral activity of Therapeutic Intervention (TI) investigates *in vitro* by therapeutic, prophylactic and virus inhibition scheme. To study the antiviral activity of TI on the model of COVID-19 virus use virus at a dose of 100 TCID50/0.2

ml. Infectivity of COVID-19 virus was calculated in accordance with the Reed-Muench method. The plates are incubated at 37 °C in 5% CO_2 for 72 hours. Six twofold dilutions of TI starting at CC_{50} were prepared to determine the inhibition efficiency of the virus by TI.

RESULTS

Results of antiviral activity of test items in the model of COVID-19 virus evaluated the presence/absence CPE in the Vero E6 cell culture. The degree of Cytopathic Effect (CPE) was calculated using the complete inhibition of cytopathic effect (CIA100) method (Figure 1).

The medical product FS-1 has virus inhibitory activity at a concentration of 3.36 mg/ml in Vero E6 cell culture against coronavirus infection COVID-19 (strain hCoV19/Kazakhstan/KazNAU-NSCEDI-481/2020) in a dose of 100 TCID50/0.2 ml (Figure 1).

Figure 1. Virus inhibition efficacy.

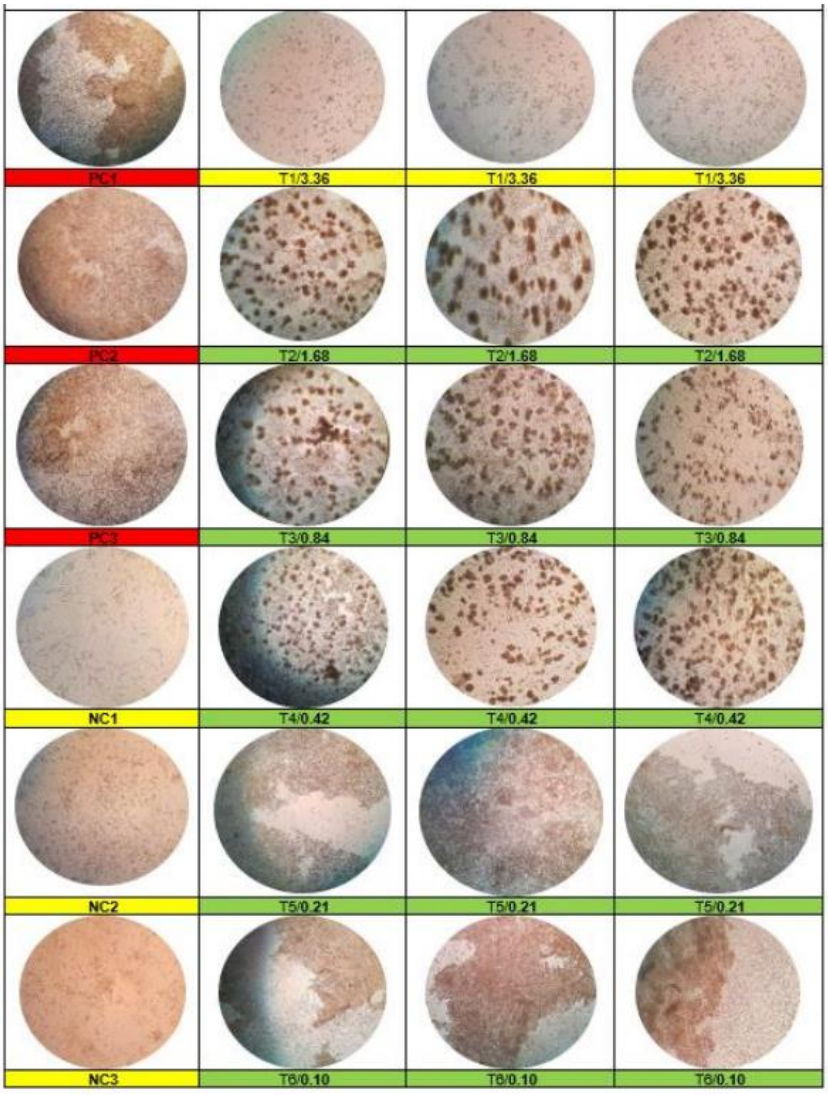

For the genome of the virus taken from isolate of SARS-CoV-2/INMI1/human/2020/ITA, the occurrence of nucleotide triplets has been analyzed. The most common triplet is AAA (281) [20].

Using DFT/B3PW91/6-31G** approach, it is shown the active complexes of drug FS-1: $(MgI_3LiI_2)^+$ and $Li(Cl)I_3$, can be segregated from the dextrin helix and can form a complex with donor-active atoms of the most common triplet AAA of viral RNA.

The structures of complexes simulating the inhibition of magnesium ions of the catalytic fragment of the ExoN domain of the nsp14 protein by the active centers of the nanocomplex of the drug FS-1: A complex of molecular iodine with lithium halide ($LiClI_2$) and a binuclear complex of magnesium and lithium with triiodide and molecular iodine (MgI_3LiII_2) have been calculated, using the DFT/B3PW91/6-31G** approach.

Complexes of active center of nanocomplex FS-1 with triplet AAA (the most common triplet) destroy the complex formed by a phosphate group of viral RNA and a catalytic fragment of domain ExoN of exoribonuclease, and form a new nucleoprotein complex where lithium chloride and $(MgI_3LiII_2)^+$ bind both viral RNA and magnesium ions of the catalytic fragment of domain ExoN of exoribonuclease. The conditions of cleavage of RNA are violated.

DISCUSSION

The structure of the active centers of the drug FS-1 and their interaction with nucleotide triplets of viral RNA

The active centers of the drug FS-1 ($(MgI_3LiII_2)^+$, $LiCl(I)I_2$) and triiodide, located inside the dextrin helix, are protected from interaction with cytoplasmic proteins by the dextrin helix and polypeptides that form coordination bonds with molecular iodine in the $(MgI_3LiII_2)^+$ complex, and hydrogen bonds with OH dextrin groups (Figures 2 and 3) [9]. With full geometry optimization, using DFT/B3PW91/6-31G** approach, total energetic and spatial complexes of $(MgI_3LiII_2)^+$, $LiCl(I)I_2$ in the dextrin ring had been obtained; in the calculations, the polypeptide was replaced by amide (I,II complexes (a,b)). The results of calculations for the $(MgI_3LiII_2)^+$, $LiII_2$ complexes are also given in our article [9].

Figure 2. Binuclear complex of magnesium and lithium, including molecular iodine and triiodide $(MgI_3LiII_2)^+$ in a dextrin ring (complex I).

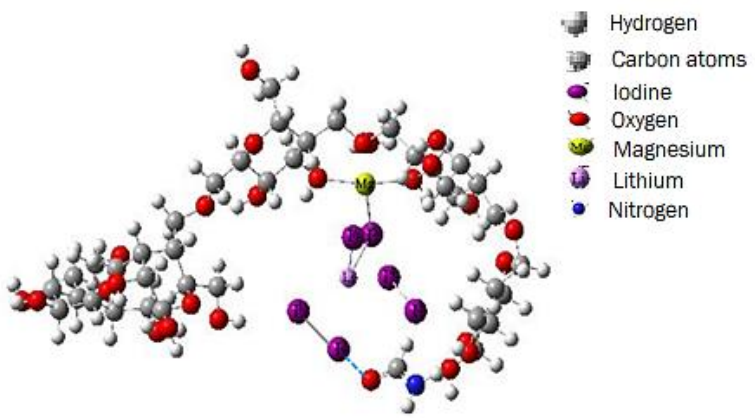

The $(MgI_3LiII_2)^+$ complex is a binuclear complex in which a magnesium ion and a lithium ion are bound by an iodine ion (I^5). Molecular iodine (I^1-I^2) is located inside the dextrin helix and is coordinated by the lithium ion and the peptide located outside the α-dextrin helix. When a magnesium ion interacts with triiodide, triiodide decomposes into iodine ion and molecular iodine (I^6-I^3 =3,54 Å, I^3–I^4=2,72 Å). However, I^3-I^4 does not have acceptor properties and cannot interact with polypeptides or DNA or RNA nucleotides. The magnesium ion is coordinated by two iodine ions and three oxygen atoms of the dextrin ring (Figure 1).

Figure 3. Complex IIa (LiClI2) in a dextrin ring.

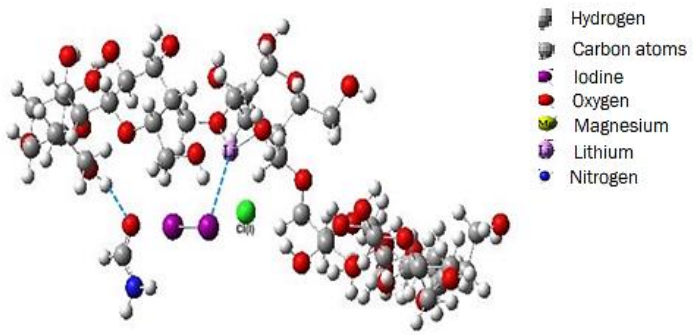

In IIa ($LiClI_2$) and IIb ($LiII_2$) complexes, the lithium ion is not on the same line with $Cl(I)I_2$, it coordinates two atoms of iodine and chlorine (or iodine) at once. This complex can be interpreted as a molecular iodine complex (I-I=2, 78 Å) with lithium ion and chlorine (or iodine) ion. When molecular iodine interacts with a chlorine ion (or iodine ion), I_2 acts as an acceptor, so a negative charge is transferred to I_2. The negatively charged molecular iodine becomes a donor to the lithium ion. The amide forms a hydrogen bond with one of the oxygen atoms of the dextrin ring and does not interact with the $LiCl\text{-}I_2$ complex (Figure 3).

Two complexes IIa ($LiClI_2$) and IIb ($LiII_2$) can be detected simultaneously in an aqueous solution of drug FS-1, since the difference in their stabilities, calculated in an aqueous solution using the COSMO model [18], is 3.67 kcal/mol.

In (I,II (a.b)) complexes, molecular iodine is in a special electronic form, not found in drugs containing iodine complexes with bioorganic ligands. In these complexes molecular iodine exhibits acceptor properties in relation to polypeptide (in complex I) or ion $Cl^-(I^-)$ (in complexes IIa.b) and donor properties-in relation to lithium ion. Probably, this electronic form of iodine provides low toxicity of the drug FS-1.

For the genome of the virus taken from the SARS-CoV-2/INMI1/human/2020/ITA isolate, an analysis of the frequency of occurrence of nucleotide triplets was performed. The most common triplet is AAA (281) [20].

We have previously established that DNA nucleotides that are more donor active towards iodine can displace the polypeptide and form a complex with molecular iodine. The interaction of active centers with DNA nucleotides is selective [9]. We have examined the possibility of segregation the $(MgI_3LiII_2)^+$, $LiCl(I)I_2$ complexes from the dextrin helix and their interaction with the donor-active atoms of the AAA nucleotide triplet of the viral RNA.

The total energies and spatial geometries complexes IIIa,b (in IIIa,b $(MgI_3LiII_2)^+$) interacts with the AAA triplet (Figure 4) and IVa,b ($LiCl(I)I_2$) interacts with the AAA triplet (Figure 5) have been calculated.

In IIIa complex formed by $(MgI_3LiII_2)^+$ with the AAA triplet, molecular iodine forms a coordination bond with the nitrogen atom of the six-membered adenosine ring, and the I-I bond breaks. Calculations have shown that the segregation of the $(MgI_3LiII_2)^+$ complex from the dextrin helix with the formation of complex IIIa is energetically favorable (ΔE=-100.37 kcal/mol). As a result of I-I bond cleavage, two ions are formed-a positively charged iodine ion and a neutral MgI_2I_2LiI fragment. The MgI_2LiII_2 fragment at the magnesium ion is coordinated by the adenosine nitrogen atom. However, the adenosine nitrogen atom is not the most donor-active atom in complex IIIa. The most donor-active atoms in this complex are the oxygen atoms of the phosphate group, so the formation of a more stable IIIb complex is possible. In complex IIIb, one oxygen atom of the phosphate group coordinates MgI_2, while LiI coordinates the other.

The positively charged iodine ion remains in the electrostatic field of the three purine bases of the triplet (Figure 4). In complexes IVa,b, molecular iodine interacts with the purine base of adenosine, and LiCl(I) is coordinated by the oxygen atom of the phosphate group (Figure 4).

The segregation of $LiClI_2$ (-7.85 kcal/mol) and LiI_3 (-9.76 kcal/mol) complexes from the dextrin helix to form complexes IVa and IVb (respectively) is energetically favorable. The energy ΔE that characterizes the difference in the stability of complexes $(MgI_3LiI_2)^+$ (complex III) and $LiCl(I)I_2$ (complex IVa,b) with a dextrin helix and with nucleotide triplet has been calculated.

ΔE is calculated as follows:

- ΔE=(Etot (IIIa,IIIb or IVa,IVb)+Etot(dex)+Etot(amid))-(Etot (I or IIa,b)+Etot(trip));
- Etot (IIIa, IIIb or IVa, IVb) is total energy of complex IIIa, IIIb or IVa,IVb,
- Etot (dex) is total energy of the dextrin ring,
- Etot (amid) is total energy of the amide,
- Etot (I, or IIa,b) is total energy of complex I, or IIa,b
- Etot (trip) is total energy of triplet.

Figure 4. Structures of complexes IIIa,b formed by $(MgI_3\ LiI_2)^+$ with the AAA triplet. (A) complex IIIa; (B) Complex IIIb.

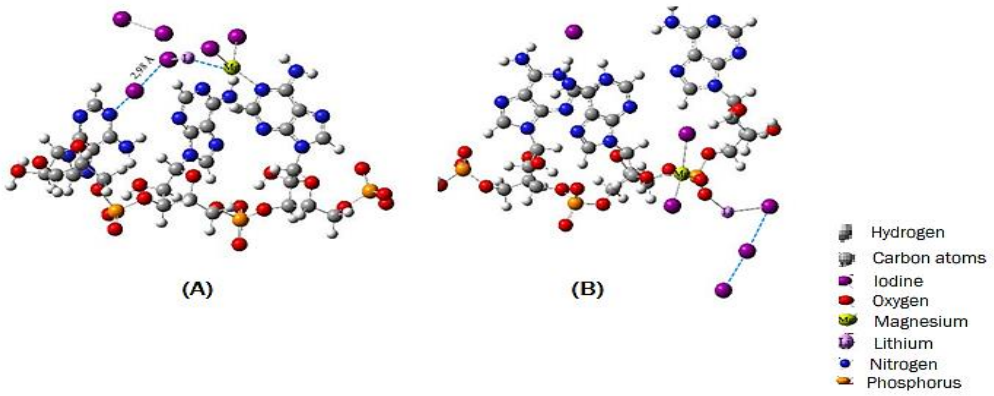

Figure 5. Structure of complex IVa formed by $LiClI_2$ with the AAA triplet (complex IVa).

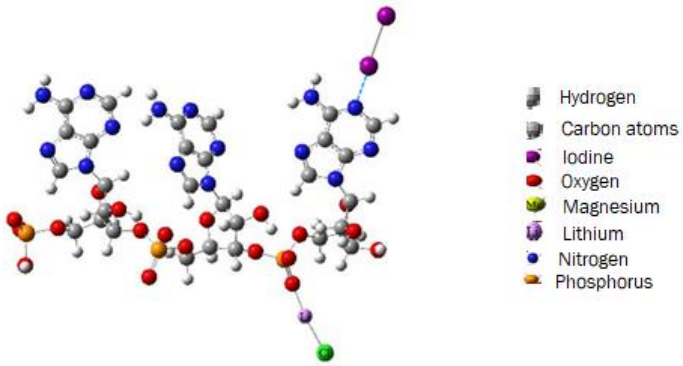

Interaction of the catalytic nucleus of domain ExoN with a phosphate group of triplet of RNA nucleotide

Non-structural protein nsp14 plays a key role in reducing the occurrence of erroneous nucleotides through its exoribonuclease domain (ExoN) [13,14]. The catalytic fragment involved in the removal of the erroneous nucleotides, domain ExoN, includes two magnesium ions that are not bound to each other in the structure of the enzyme. They are bound into the binuclear complex only when interacting with a phosphate group of virus's RNA triplet.

The model of interaction between two magnesium ions of the catalytic fragment and a phosphate group is presented in the article [15]. Two magnesium ions are surrounded by five amino acid residues DEDDh, which create the electrophilic environment required to fix the two ions to the ligands involved in the catalysis and to cleave RNA. One magnesium ion is coordinated by the amino acid residues of glutamic and aspartic acids, and the second one is coordinated by amino acid residue of aspartic acid. It is also noted that the presence of a water molecule is required for the catalysis.

The spatial and electronic structure is calculated for complex V (Figure 6) formed by binuclear catalytic fragment of domain ExoN and a phosphate group at nucleotide triplet of virus with the erroneous nucleotide (for example, AGA). In calculations, the hydrocarbon fragment of aspartic and glutamic acids has been replaced by a CH_3 group (Figure 6). As seen in Figure 6, two magnesium ions are coordinated by two oxygen atoms of a phosphate group. One magnesium ion is coordinated by amino acid residue of glutamic acid, while the other is coordinated by amino acid residue of aspartic acid and a water molecule. The two ions are bound by amino acid residue of aspartic acid. It is possible that the magnesium ions unbound between themselves in the structure of domain ExoN do not approach the phosphate group simultaneously.

It can be assumed that complex V is formed in two stages. Initially, more stable complex VI is formed where the phosphate group interacts with a positively charged magnesium complex: A magnesium ion is coordinated by amino acid residue of aspartic acid and a water molecule. Then, complex VI interacts with a neutral magnesium complex, in which a magnesium ion is coordinated by two amino acid residues of aspartic and glutamic acids.

The amino acid motif of the catalytic nucleus contains five amino acids DEDDh. Our calculations have shown that two amino acid residues of histidine and aspartic acids are not involved in the complex formation of magnesium ions and a phosphate group. Based on the catalysis model proposed in the articles [16,17]. for super-family exonucleases such as e-sub-unit of DNA of polymerase III of *E. coli*, one can assume that these two amino acid residues are involved in cleavage of RNA.

Figure 6. The structure of complex V, formed by the binuclear catalytic fragment of the ExoN domain and a phosphate group in a nucleotide triplet with an erroneous nucleotide (for example, AGA) and the structure of the intermediate complex VI, in which the phosphate group interacts with a positively charged magnesium complex: A magnesium ion coordinated by an amino acid residue of asparagine and a water molecule. (A) Complex V; (B) Complex VI.

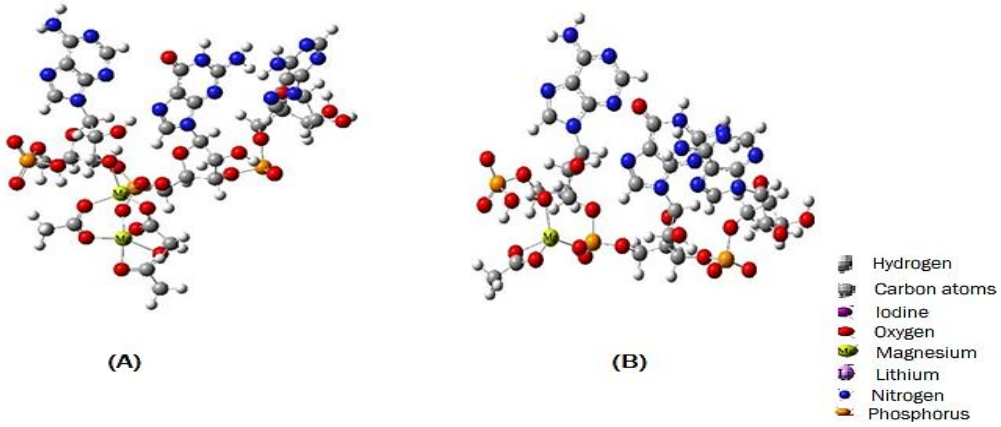

Inhibition of two magnesium ions of the catalytic fragment of the ExoN domain by lithium chloride and by complex of AAA triplet with $(MgI_3\ LiI_2)^+$

Magnesium ions are not interconnected in the structure of the ExoN domain, so they can be bound and complexed independently by the active centers of the drug FS-1.

Energy of interaction of VI complex with the second magnesium ion ($MgAspH_2O$) ($\Delta E1$=-37.9 kcal/mol) and VI complex interaction energy with lithium chloride ($\Delta E2$=-57.18 kcal/mol) and with lithium iodide ($\Delta E3$=-20.09 kcal/mol). The formation of complex VII, in which it is not the second magnesium ion that interacts with complex VI, but lithium chloride, is the most energetically favorable. These calculations allowed us to consider the possibility of inhibition of complex VI by lithium chloride bound to the phosphate group in complex IVa.

Calculations have shown that the binding energy of lithium chloride with the phosphate group in complex IVa, formed by $LiCII_2$ with the AAA triplet, (-51.71 kcal/mol) is less than the binding energy of lithium chloride with complex VI (-57.17 kcal/mol); therefore, LiCl can move from the AAA triplet nucleotide to complex VI with the formation of complex VII (Figure 7).

Figure 7. Structure of complex VII formed by lithium chloride with a phosphate group and $MgAspH_2O$ ion (Complex VII).

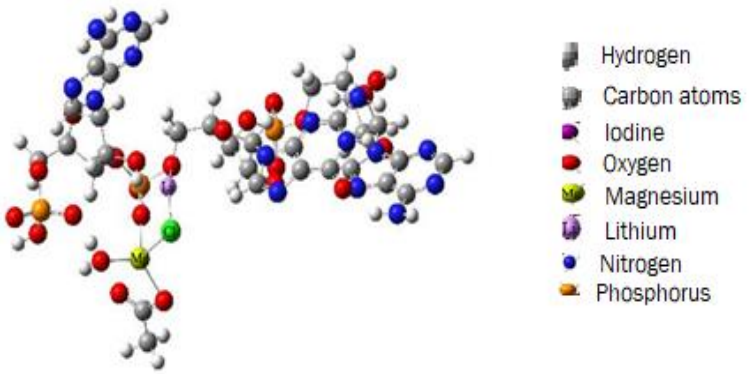

Thus, lithium chloride displaces the second magnesium ion from the catalytic complex V and binds the positive magnesium complex, coordinated by the amino acid residue of aspartic acid and a water molecule. This is complex VII (Figure 7).

The second neutral magnesium complex, coordinated by the amino acid residues of aspartic and glutamic acids, of the catalytic fragment can be coordinated by donor-active complex IIIb to form complexes VIII (Figure 8).

Figure 8. Inhibition of the neutral magnesium complex of the ExoN, coordinated by aspartic and glutamine amino acid residues, by the active center $(MgI_3LiII_2)^+$ (Complex VIII).

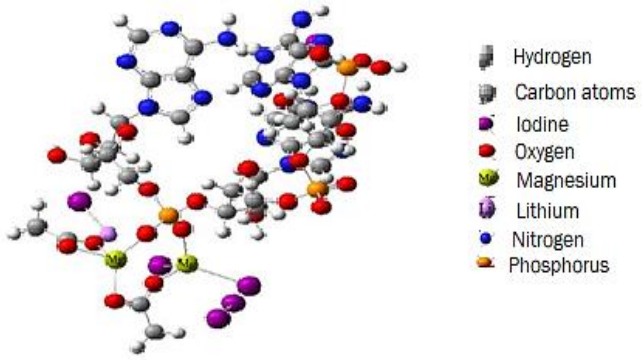

Complex IIIb is rearranged upon interaction with the neutral magnesium complex. In complex VIII, the neutral magnesium complex is coordinated by the oxygen atom of the phosphate group and the $(MgI)I_3$ ion. The oxygen atom of aspartic acid coordinates LiI.

Thus, $Li(Cl)I_2$ and $(MgI_3LiI_2)^+$ destroy the complex formed by the phosphate group of the viral RNA and the catalytic fragment of the ExoN exoribonuclease domain, and create a new nucleoprotein complex in which lithium chloride and $(MgI_3LiII_2)^+$ bind both the viral RNA and the magnesium ions of the catalytic fragment. The conditions ensuring the cleavage of viral RNA are disturbed.

CONCLUSION

The drug FS-1 has virus inhibitory activity at a concentration of 3.36 mg/ml in Vero E6 cell culture against coronavirus infection COVID-19 (strain hCoV19/Kazakhstan/KazNAU-NSCEDI-481/2020) in a dose of 100 TCID50/0.2 ml.

The active centers of the drug FS-1 ($(MgI_3LiII_2)^+$, $LiCl(I)I_2$), located inside the dextrin helix, are protected from interaction with cytoplasmic proteins by the dextrin helix and polypeptides that form coordination bonds with molecular iodine in the complex $(MgI_3LiII_2)^+$ and hydrogen bonds with the OH groups of dextrin.

For the genome of the virus taken from the SARS-CoV-2/INMI1/human/2020/ITA isolate, an analysis of the frequency of occurrence of nucleotide triplets was performed. The most common triplet is AAA (281). It has been shown that the MgI_3LiII_2 and $LiClI_2$ complexes can be segregated from the dextrin helix and form a complex with the donor-active atoms of the AAA triplet of the viral RNA (complexes IIIa,b (AAA MgI_3LiII_2) and IVa (AAA $LiClI_2$), IVb (AAA LiI_3)).

The structures of complexes simulating the inhibition of magnesium ions of the catalytic fragment of the ExoN domain of the nsp14 protein by the active centers of the nanocomplex of the drug FS-1: A complex of molecular iodine with lithium halide ($LiClI_2$) and a binuclear complex of magnesium and lithium with triiodide and molecular iodine (MgI_3LiII_2) have been calculated.

We calculated the spatial and electronic structure of the complex formed by the binuclear catalytic fragment of the ExoN domain and the phosphate group in the nucleotide triplet of the virus with an erroneous nucleotide (for example AGA) with full geometry optimization.

It is possible that magnesium ions, unbound to each other in the ExoN domain structure, do not approach the phosphate group simultaneously. It can be assumed that complex V is formed in two stages. First, a more stable complex VI is formed, in which the phosphate group interacts with a positively charged magnesium complex–a magnesium ion coordinated by aspartic acid and a water molecule. Complex VI then interacts with the neutral magnesium complex and created complex V.

The interaction energies of complex VI with the second magnesium ion (ΔE1=-37.9 kcal/mol), complex II with lithium chloride (ΔE2=-57.18 kcal/mol) and with lithium iodide (ΔE3=-20.09 kcal/mol) have been calculated. The formation of complex VII, in which it is not the second magnesium ion that interacts with complex VI, but lithium chloride, is the most energetically favorable.

The binding energy of lithium chloride in complex IVa (-51.71 kcal/mol) is less than the binding energy of lithium chloride with complex VI (-57.17 kcal/mol); therefore, LiCl can move from the nucleotide triplet AAA to complex VI to form a complex VII.

Lithium chloride displaces the second magnesium ion from the catalytic complex V and binds the positive magnesium complex (complex VI), coordinated by the amino acid residue of aspartic acid and a water molecule. The conditions ensuring the viral RNA cleavage are disturbed.

The displaced magnesium ion can be inhibited by the complex formed by the nucleotide triplet AAA with MgI_3LiII_2.

Thus, $Li(Cl)II_2$ and $(MgI_3LiII_2)^+$ destroy the complex formed by the phosphate group of the viral RNA and the catalytic fragment of the ExoN exoribonuclease domain and create a new nucleoprotein complex in which lithium chloride and $(MgI_3LiII_2)^+$ bind both the viral RNA and the magnesium ions of the catalytic fragment.

AUTHORS' CONTRIBUTIONS

Created a molecular model inhibition of the catalytic fragment of domain ExoN of exoribonuclease of virus SARS-CoV-2-betacoronavirus B by complexes containing molecular iodine and lithium and magnesium halides GAY; experimentally discovered that complexes containing molecular iodine and lithium and magnesium halides (the drug FS-1) substance has virus inhibitory activity at a concentration of 3.36 mg/ml in Vero E6 cell culture against coronavirus infection COVID-19 (strain hCoV19/Kazakhstan/KazNAU-NSCEDI-481/2020) in a dose of 100 TCID50/0.2 ml ISK and KT and KT; created the drug FS-1 AII; All authors read and approved the final manuscript.

FUNDING

The study was supported by the grant BR24992760 Development of potentiator for antimicrobial action of antibiotic combinations for effective therapy of diseases caused by multi-drug resistant bacteria.

ACKNOWLEDGMENT

The calculations were made on the Computing Cluster of the National Scientific Laboratory for the collective use of Information and Space Technologies at KazNITU K.I. Satpaeva.

REFERENCES

1. Eltayb WA, et al. Novel investigational anti-SARS-CoV 2 agent Ensitrelvir “S-217622”: A very promising potential universal broad-spectrum antiviral at the therapeutic frontline of coronavirus species. ASC Omega. 2023;6:5139-6125.

2. Chien M, et al. Nucleotide analogues as inhibitors of SARS-CoV-2 polymerase, a key drug target for COVID-19. J Proteome Res. 2020;19:4690-4697.
3. Ilin A, et al. Action mechanism of molecular iodine complex with bioorganic ligands, magnesium and lithium halogenides on human tuberculosis strain with multiple drug resistance. J Microbiol Biochem Technol. 2017;9:293-300.
4. Yuldasheva G, et al. Quantum-chemical model of the inhibition HIV-1 intergrase action by iodine complex compounds and lithium halogenides. J AIDS Clin Res. 2015;6:2-6.
5. Yuldasheva G, et al. Molecular modeling of the anti-HIV activity mechanism of iodine-containing drugs armenicum and FS-1. ACS Omega. 2023;8:8617-8624.
6. Ilin A6 Kulmanov M. Antibacterial agent for treating infectectious diseases of bacterial origin. U.S. Patent 2010. [Google Scholar]
7. Yuldasheva G, et al. Iodine Containing Drugs: Complexes of Molecular Iodine and Tri-Iodide with Bioorganic Ligands and Lithium Halogenides in Aqueous Solutions. In: Leszczynski J, Shukla M (eds) Practical aspects of computational chemistry IV. Springer, Boston, USA. 2016;279-301.
8. Yuldasheva G, et al. Effect of organic ligands with conjugated π-Bonds upon the structure of iodine-α-dextrin complexes. Biotechnol Appl Biochem. 2012;59:29-34.
9. Yuldasheva G, et al. Structure of the active nanocomplex of antiviral and anti-infectious iodine-containing drug FS-1. Quantum Rep. 2021;3:746-812.
10. Gorbalenya A, et al. Nidovirales: Evolving the largest RNA virus genome. Virus Res. 2006;117:17–37.
11. Chen Y, et al. Emerging coronaviruses: Genome structure, replication, and pathogenesis. J Med Virol. 2020;92:418-423.
12. Fehr AR, et al. Coronaviruses: An overview of their replication and pathogenesis. Methods Mol Biol. 2015;1282: 1-23.
13. Bouvet M, et al. RNA 3′-end mismatch excision by the severe acute respiratory syndrome coronavirus nonstructural protein nsp10/nsp14 exoribonuclease complex. Proc Natl Acad Sci USA. 2012;109:9372–9377.
14. Graham R, et al. A live, impaired-fidelity coronavirus vaccine protects in an aged, immunocompromised mouse model of lethal disease. Nat Med. 2012;12:1820-1826.
15. Ma Y, et al. Structural basis and functional analysis of the SARS coronavirus nsp14–nsp10 complex. PNAS 2015;112: 9436-9441.
16. Hamdan S, et al. Structural basis for proofreading during replication of the *Escherichia coli* chromosome. Structure. 2002;10:535-546.
17. Beese L, et al. Structural basis for the 3' 5' exonuclease activity of *Escherichia coli* DNA polymerase 1: A two metal ion mechanism. EMBO J. 1991;10:25-33.
18. Klamt A, et al. COSMO: A new approach to dielectric screening in solvents with explicit expressions for the screening energy and its gradient. J Chem Soc. 1993;2:799-805.
19. Frisch M, et al. Gaussian 09 citation. Wallingford: Gaussian Inc., United Kingdom. 2009.
20. National Center for Biotechnology Information (NCBI). Bethesda (MD): National Library of Medicine (US). 1988.